H. Performance Evaluation and Durability Prediction of Dissimilar Material Hybrid Joints

D. L. Erdman
Oak Ridge National Laboratory
P.O. Box 2009, Oak Ridge, TN 37831-8048
(865) 574-0743; fax: (865) 574-8257; e-mail: erdmandl@ornl.gov

Field Project Manager: C. David Warren
Oak Ridge National Laboratory
P.O. Box 2008, Oak Ridge, TN 37831-8050
(865) 574-9693; fax: (865) 574-0740; e-mail: warrencd@ornl.gov

Technology Area Development Manager: Joseph A. Carpenter
(202) 586-1022; fax: (202) 586-1600; e-mail: joseph.carpenter@ee.doe.gov
Field Technical Manager: Philip S. Sklad
(865) 574-5069; fax: (865) 576-4963; e-mail: skladps@ornl.gov

---

Contractor: Oak Ridge National Laboratory
Contract No.: DE-AC05-00OR22725

Objective

- Develop new experimental methods and analysis techniques to enable hybrid joining as a viable attachment technology in automotive structures. This will be accomplished by evaluating the mechanical behavior of composite/metal joints assembled using a variety of hybrid joining methods and quantifying the resulting damage mechanisms under environmental exposures, including temperature extremes and automotive fluids, for the ultimate development of practical modeling techniques that offer global predictions for joint durability.

Approach

- Characterize the structural hybrid joint to quasi-static load conditions.
- Characterize response to fatigue, creep, and environmental exposures.
- Conduct predictive analysis.

Accomplishments

- Developed new procedures for manufacturing adhesive coupon specimens to eliminate undesirable voids during processing; the voids resulted in inconsistent material properties.
- Completed static and time-dependent testing of the adhesive for modeling input parameters.
- Implemented new adhesive material properties in the structural rail models and assessed the sensitivity of the adhesive time-dependent behavior on overall structural response.
- Evaluated basic damage modeling techniques employing finite-element method (FEM) analysis to improve predictive modeling accuracy.

- Evaluated the fundamental mechanical properties of the newly acquired Quantum carbon composite material at the coupon level.
- Carried out quasi-static, fatigue, and creep testing of hybrid rail joints composed of Quantum carbon composite.
- Completed cold testing (–40ºC) of the Quantum carbon composite hybrid rail specimens.

Future Direction

- Continue to explore the material nonhomogeneity of the Quantum carbon composite and evaluate the influence on structural behavior and ramifications related to predictive modeling.
- Develop damage modeling schemes to enhance hybrid joint durability predictions.
- Explore methods to develop fatigue life predictions in hybrid joints.

Introduction

Weight can be reduced and fuel efficiency increased in automobiles, without compromising structural integrity or utility, by incorporating innovative designs that strategically utilize modern lightweight materials—such as polymeric composites—in conjunction with traditional structural materials such as aluminum, magnesium, and steel. Despite the advantages associated with such dissimilar or hybrid material systems, there is reluctance to adopt them for primary structural applications. In part, this reluctance can be attributed to the limited knowledge of joining techniques with such disparate materials where traditional fastening methods such as welding, riveting, screw-type fasteners, and bolted joints may not be appropriate.

One solution to this problem is the use of hybrid joining techniques by which a combination of two or more fastening methods is employed to attach similar or dissimilar materials. One example is a mechanically fastened joint (i.e., bolted or riveted) that is also bonded with adhesive. These types of joints could provide a compromise between a familiar mechanical attachment that has proven reliability, and the reduction of problematic issues such as stress concentrations and crack nucleation sites introduced by using mechanical fasteners with polymeric composites.

The use of hybrid joining could also lead to other potential benefits such as increased joint rigidity, contributing to overall stiffness gains and a reduction of vehicle mass. Additionally, the use of adhesives in conjunction with mechanical fasteners could significantly reduce stress concentrations, which serve as locations for crack starters. Hybrid joining methods can also provide additional joint continuity to allow increased spacing between fasteners or welds.

Although numerous benefits are derived from using hybrid joining techniques, and the joining of dissimilar materials is becoming a reality, little or no practical information is available concerning the performance and durability of hybrid joints. Therefore, this project has taken on the task of developing new technologies to quantify joint toughness and predict long-term durability. This will necessitate identifying and developing an understanding of key issues associated with hybrid joint performance, such as creep, fatigue, and effects of environmental exposure.

To initiate this study, it was necessary to choose a candidate hybrid joint representative of those typically encountered in automobiles. Because of their wide applicability in automotive structures, several

combinations of hat-section geometries were considered. Hat-sections can be incorporated into a variety of generic automotive structural components, such as crush-tubes or frame rails, when they are bonded and mechanically fastened to other geometries. For the current study, the Joining Task Force selected a composite hat-section bonded and riveted to a steel base, as shown in Figure 1. This selection was made on the basis of general applicability to a variety of automobile structural components. Members of the Joining Task Force identified industry partners for sources for the steel, rivets, composite hat-section, and adhesive.

To determine the influences of the adhesive and the rivets on the structural performance of the rail, it was also decided to investigate bonded specimens without rivets and riveted specimens without adhesive.

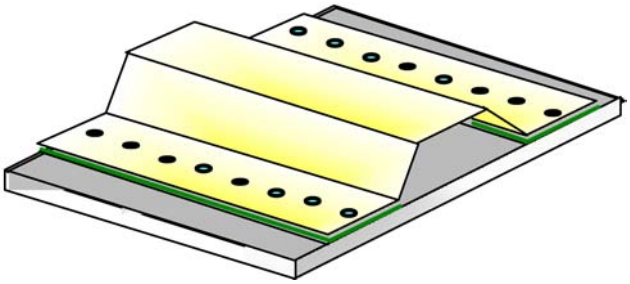

Figure 1. Hybrid joint schematic.

Adhesive Processing Refinement and Re-evaluation of Adhesive Material Properties

Although tensile testing of the 654ETG adhesive was carried out at the start of this project, comparisons of the results with recent tests of the same material in another lightweighting materials project [Energy Absorption in Adhesively Bonded Structures (7E)] revealed inconsistencies in the stiffness, strengths, and relative scatter between the two data sets. The fracture surfaces of suspect specimens that exhibited lower than average strength and/or stiffness often showed large voids created by trapped air introduced during the molding process. The voids are easily discernable with the naked eye (Figure 2). Effectively, the bubbles in the material provide crack starter sites and reduce the cross-sectional area of the specimen, resulting in the inconsistencies mentioned. To eliminate this problem, a new procedure was developed to deposit the highly viscous adhesive onto the molding platens after centrifuging it to remove any air introduced during mixing. Any manipulation of the adhesive that would result in shearing or creating tension was eliminated, and only compressive forces were used to distribute the adhesive to fill the mold. Machining of the specimens from plaques molded in this manner revealed much more homogeneous, void-free specimens. Posttest examination of the fracture surfaces indicated failure of the material that was not initiated from voids in the material, resulting in much more consistent stress-strain behavior (Figure 3 and Table 1). This processing technique was adopted for use in all tensile and creep test specimen preparation.

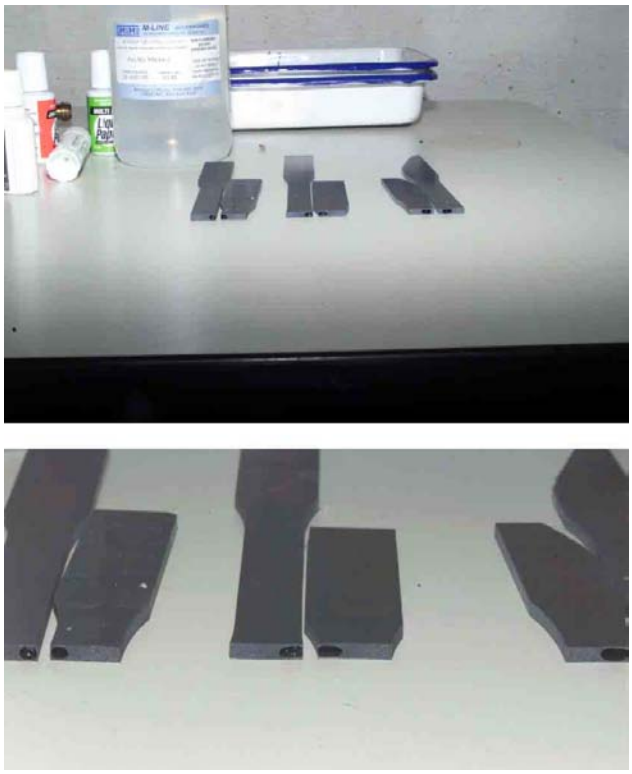

Figure 2. Internal bubbles/voids on tensile specimen fracture surfaces contributed to inconsistent scatter in material properties.

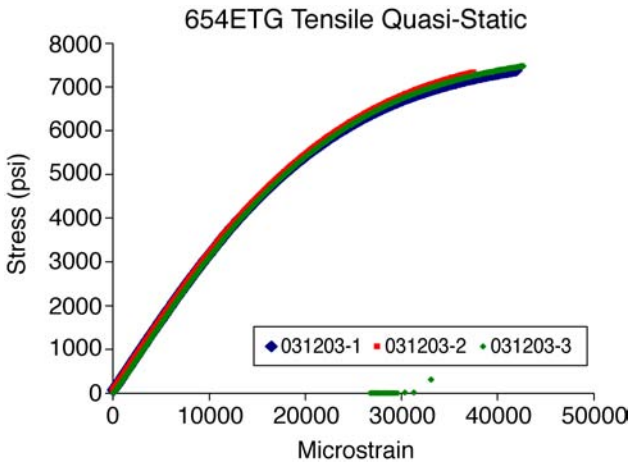

Figure 3. Typical stress-strain curves with the new specimen processing techniques reduced scatter.

Table 1. Static test results for tensile tests plotted in Figure 3

	Strength (ksi)	Modulus (Msi)
	7.378	0.3274
	7.332	0.3268
	7.476	0.3262
Average	7.395	0.3268
Standard deviation	0.073	0.0006

Adhesive Creep Testing

Because of the time-dependent response of adhesives under constant load, we needed to establish the sensitivity of the rail specimens to adhesive creep for the modeling effort. The first step was creep testing of tensile specimens to determine strain accumulation over time. Typical creep curves are plotted in Figure 4. Although there is noticeable scatter in the curves (variation in strain levels despite identical stress levels for all specimens) these data could be used within the FEM model to determine if the creep response of the adhesive contributed significantly to the overall response of the rail. The creep data in Figure 4 were curve-fit with a standard power-law representation suitable for the FEM program (ABAQUS) input:

$$\varepsilon_{creep} = C\sigma t^{n}$$

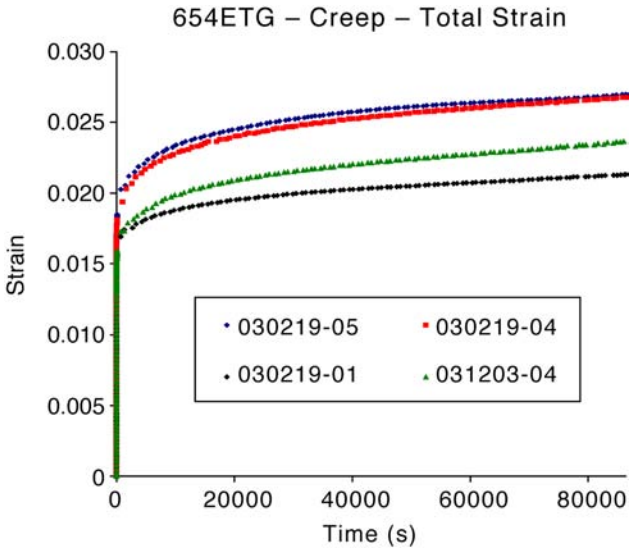

Figure 4. Creep test data for four specimens conducted at 60% of failure stress show noticeable scatter.

where

ε_{creep} = creep strain
σ = applied stress
t – time
C,n = power law coefficients

Because the applied stress and the time are known test parameters, simple curve-fitting techniques were used to determine the coefficients for the power law. The creep strain, which increases with time, was added to the instantaneous strain obtained at the start of the test to obtain the total strain. This information was then used as input in the rail model, with similar creep properties for the composite supplied by the Composite Durability Project. The complete rail was then analyzed in three runs, considering only creep of the adhesive, only creep of the glass composite, and creep behavior for both the composite and the adhesive. Although the adhesive alone exhibits significant creep response, the effect is negligible on the overall rail response. However, including the creep response of the glass composite results in substantial creep of the rail. This result indicates that the additional computation to

include the creep response of the adhesive is unnecessary and can be omitted in future model development. When the model results were compared with results of a creep test on a glass-composite rail specimen, large discrepancies were evident. This is not surprising, considering the level of damage observed during the test (tearing of the composite was obvious) that was not included in the current model. Therefore, damage needs to be introduced into the model. Note, however, that the test on the rail specimen was run at 85% of failure load, which resulted in the large damage accumulation indicated by the periodic jumps in strain level over time. Better agreement may exist at lower levels of creep loading. This issue will be studied with the new Quantum carbon material being procured for rest of this project.

Preliminary Damage Modeling

Three types of exploratory damage models were implemented in ABAQUS to explore the existing capabilities of the FEM program and initiate the introduction of damage into the existing modeling scheme. All three damage models are smeared in that individual cracks are not included; instead, reduction in material stiffness properties is simulated. Hence, the packaged damage capabilities simulate global degradation of material properties. The simplest analysis, which assumed the composite to be perfectly plastic, was performed primarily for comparison with the following two models. The other two models attempt to simulate experimentally observed brittle behavior. Both models predict material softening to occur after a certain stress level is attained. The softening is defined by either a stress-strain relationship or a stress-displacement relationship. In certain situations, the simpler strain softening may produce undesirable mesh sensitivity, yielding indistinct results for the same structure, or may not converge at all. The displacement-softening model avoids this difficulty; however, additional restrictions are placed on the mesh, limiting the analysis.

A typical mesh used for modeling is depicted in Figure 5. It is obvious that the global damage analysis routines packaged with ABAQUS are inadequate to model the extensive tearing of the composite material that was observed experimentally and will need to be addressed with some other user-defined subroutines slated for development in FY 2004.

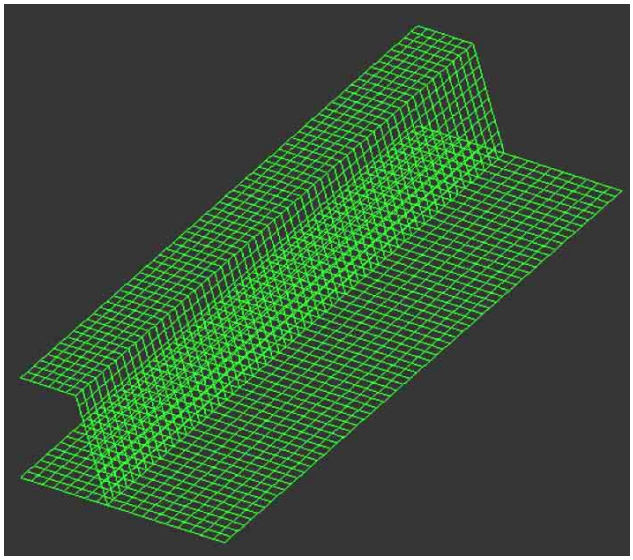

Figure 5. Typical mesh used to model the hybrid joint.

Mechanical Hybrid Rail Studies with Quantum Carbon Composite Material

In the second half of FY 2003, the selected composite material for the hybrid rail structure was introduced. Because the new material had not been characterized at Oak Ridge National Laboratory, coupon specimens were tested to evaluate basic material properties; this was in addition to testing of the structural hybrid rail specimens consisting of new composite hat sections bonded to steel base plates. Large scatter in the coupon tensile properties was observed for the Quantum material, which poses a new challenge in evaluating the failure mechanisms witnessed during the bending tests on hat sections. This scatter led

to a thorough investigation of the composite materials properties unanticipated at the onset of this work.

As previously, the composite hat sections were joined to metal sheet bases by riveting, adhesive bonding, or a combination of the two. All testing was conducted in the same manner as for the swirled glass hat specimens. Bending fixtures, data acquisition software, and experience acquired from the glass specimen tests helped accelerate the testing of Quantum specimens over the last 6 months of FY 2003. Replicate tests were conducted for each hybrid rail specimen in the three joining configurations in quasi-static mode at room temperature and low temperature (–40°C). In addition, fatigue and creep testing at room temperature provided additional information for predictive modeling efforts.

Static Coupon Properties of Quantum Composite Material

Coupon tensile testing was performed on the Quantum material, which was also used for the latest set of hat section specimens making up the hybrid joint rail under consideration. Exploratory tensile testing of flat coupon specimens showed substantial variations in stiffness and strength. Therefore, many tests were required to statistically quantify the material properties being observed to provide reasonable material properties for FEM predictions in the structural modeling of the rails.

Stiffness was measured on 0.5-in.-wide tensile specimens using an extensometer with 1-in. gage length. Stiffness varied among replicate specimens, as well as at various locations on a single specimen, because the extensometer location on a single specimen indicated a high level of nonhomogeneous material behavior. Incremental loading tests were carried out by subjecting the specimen to monotonically increasing load cycles to observe a global indication of damage progression through reduction of stiffness. Tensile coupons were loaded in 200-lb increments, and stiffness was measured by three checks after each loading cycle. A modest decrease in Young's modulus was observed through a general decrease in specimen stiffness with increased load level. This inconclusive reduction in stiffness may be attributed in part to the nonhomogeneous properties of the material.

Hybrid Rail Joint Testing

In conjunction with the tensile testing of the Quantum material at the coupon level, we conducted quasi-static, fatigue, and creep tests of the hybrid rail specimens to assess their mechanical performance and validate future modeling endeavors. Joining methods were consistent with earlier rail tests conducted primarily on swirled glass hat specimens. The specimens joined via adhesive bonding, riveting, and a combination of the two were revisited. The loading conditions were also adopted from previous studies with the hat section being loaded in both tension and comprehension.

Quasi-Static Tests at Room Temperature

Three replicate specimens were tested for each combination of loading (tension and compression) and the three joint configurations. Two of the three replicate tests were instrumented with linear variable differential transformers (LVDTs) for the case of the hat section in tension, and a single displacement gage for the case of the hat in compression. The results from these displacement measurements will be used to correlate with the predicted displacements from analytical models.

Damage and failure behavior observed during the quasi-static tests of the Quantum hat section specimens was somewhat similar to previous test specimens consisting of swirled-mat-glass hat sections; this indicates the damage characteristics are probably dictated more by the geometry of the specimen than the composite material.

The specimens tested in compression exhibited slight degradation in stiffness and almost no discernible damage until the composite flanges catastrophically separated from the metal base of the hat-section at the location of contact with the support rollers. At this point a discernable drop in load occurs as shown in Figure 6. This first step in the failure process was also accompanied by a saddlelike deformation of the steel base, which became more pronounced as the load increased up to failure, indicating large-scale plastic deformation of the steel. As the failure process progressed from the initial drop in load due to the rapid failure at the flanges, continuous longitudinal tearing of flanges occurred, extending from the initial flange to the steel separation point and continuing to grow until the final specimen failure.

For hat section specimens in tension, catastrophic failure occurred at the top of the hat section and remained solely in the composite material. The crack was often located away from the longitudinal center of the specimen, where the bending stresses are the greatest, and is most likely attributable to the variation of properties in the Quantum composite material. Hence, the specimen is failing at a location where the stresses are lower but where the material strength is also lower.

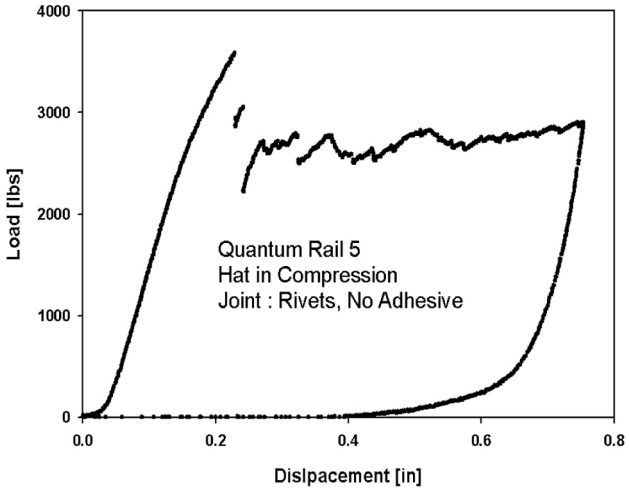

Figure 6. Typical load displacement curve indicating longitudinal tearing of flanges for hat loaded in compression during quasi-static test.

Only two specimens sustained significant push-through damage caused by contact stresses from the rollers that would influence the load-displacement behavior. In previous tests on glass composite specimens, there was a completely different failure process between the specimens that were adhesively bonded and those that were riveted. In the case of glass specimens with rivets only, cracking initiated from the location of the roller contact points, and failure occurred in the flange. Glass specimens bonded with adhesive failed in the composite at the top of the hat. In contrast, the Quantum specimens joined solely with rivets or adhesive specimens exhibited only catastrophic failure of the composite hat section with no preliminary damage in the flange region prior to failure.

Table 2 summarizes briefly the relative strengths measured in the tests of the Quantum rail specimens. Note that, for tests with the hat in tension or compression, the loads attained are consistently higher for joints that are both bonded and riveted. This suggests a single joining method may be inferior to hybrid joints using both mechanical attachment and adhesive bonding.

Table 2. Average maximum load (lb) obtained from three sets of quasi-static tests

Average maximum load (lb)	Tension	Compression
Rivets and adhesive	4044	4183
Rivets	3099	3501
Adhesive	3820	3497

Fatigue Testing

Fatigue tests were performed at 70% of ultimate load determined from the average of the quasi-static tests for each loading/joint attachment configuration. As with most S-N fatigue testing, an order of magnitude difference was observed in the number of cycles to failure for replicate fatigue tests. Specimens failing at fewer cycles generally sustained damage comparable to the specimens tested in quasi-static mode, indicating weak regions

in the hat sections. This result was not surprising considering the nonhomogeneity of the composite and variability of composite strength and stiffness among the various specimens. Specimens failing at higher cycle counts exhibited extensive progressive damage, including multiple rivet failures, widespread adhesive cracking, and cracks originating from rivet holes that developed and grew in the metal base of the specimen prior to failure.

This failure behavior is consistent with the large variation in properties in the Quantum material and can be described by the following scenario. When highly stressed areas of the specimen coincide with weak material areas in the composite hat, the hat failed in these regions as in the quasi-static tests. When the material in highly stressed areas of the hat was strong enough to sustain the fatigue loading without immediate failure, other components of the structure failed and redistributed the stresses, enabling the structure to sustain a much higher level of damage before collapsing. Examples of these types of extensive damage are shown in Figures 7 and 8, where numerous rivet pull-outs and extensive cracking of the metal base can be seen observed without difficulty.

Figure 7. Broken and missing rivets—riveted specimen failed after 30,000 cycles at 70% of static ultimate load with the hat in compression.

Creep Testing

A complete permutation of the three specimen types and the two loading conditions was included in the creep test matrix.

Figure 8. Cracking of metal during fatigue test—adhesively bonded specimen.

Specimens were tested for creep at 40% of ultimate load to avoid large-scale damage because the viscoelastic response of the material was needed for modeling efforts that currently do not contain damage analysis. There was no visible damage on the Quantum hats, although some imprints from the rollers were detectable in the metal part of the structure; also, minor matrix cracking could be heard on initial loading for some specimens, indicating minimal damage in the composite. Hence, the time-dependent increase in displacements recorded throughout the creep test was thought to be a result of material response and not an artifact of extensive damage, which would be indicated by large jumps in displacement at intermittent points in the test. The level and significance of any indiscernible damage could possibly be estimated by evaluating the residual deformation after unloading and comparing the test results with time-dependent FE simulations, which do not include damage. Comparisons of the creep results with FEM models are under way.

Cold Static Testing

A set of quasi-static tests was carried out at –40°F. A Styrofoam environmental chamber designed in-house was cooled with liquid nitrogen to the desired temperature and then allowed to reach equilibrium. The test was then carried out in a manner identical to the quasi-static test at room temperature. The major difference in the results for cold

testing was an increase in the load at failure at –40°F, which significantly exceeded the average load values obtained at room temperature. Bond failure was observed for some adhesively bonded specimens; however, it is unclear if the failure occurred during the test or after the composite failure, because the specimen could not be visually observed during the test because of the chamber design. The increase in strength in the cold condition may be attributable to an increase in the stiffness of the composite material, leading to smaller displacements possibly accompanied by a higher yield point in the steel. The cold environment did not appear to have a detrimental effect on the strength of the structure. Strength results for these tests are listed in Table 3 (see Table 2 for room-temperature results).

Table 3. Maximum load (lb) for quasi-static tests at –40°F

Maximum load (lb)	Tension	Compression
Rivets and adhesive	4662	4497
Rivets	3531	4000
Adhesive	3774	4805

Conclusions

New methods of manufacturing specimens were developed to enable the collection of test data on material properties of the adhesive in a hybrid rail structure. Because these properties are used as inputs to FEM modeling, consistent data are necessary to ensure accuracy in model predictions.

Our study of creep behavior in the hybrid rail revealed that the effects of creep in the adhesive have little or no effect on the global response of the structure and can be omitted from the analysis. However, the creep behavior of the composite drastically affects the behavior of the rail and should be included in the modeling scheme.

Exploratory testing with the damage routines included with the FEM package found them inadequate to model the complex cumulative damage observed experimentally in the hybrid rail specimen. This inadequacy will need to be addressed in the next phase of the modeling, possibly with the implementation of user-defined subroutines.

In general, significant differences between Quantum composite material and the glass composites studied earlier were observed in virtually all aspects of the test program. Tensile testing at the coupon level revealed large levels of scatter in material strength and stiffness. In addition to the scatter in properties among replicate specimens, we discovered that the material is highly nonhomogeneous in composition. There are regions of randomly occurring variation in properties, including strength and stiffness, throughout the material. This nonhomogeneity not only is observable at the coupon level but also has evident effects on the structural response of the hybrid rail specimens constructed from the composite hat sections. One of the greatest concerns associated with this material feature is its effect on fatigue life: two random samples of the material can exhibit completely different fatigue behaviors. The first is a number of short-lived cycles to failure with a simple nonprogressive damage pattern similar to that observed in quasi-static loading tests if the sample is from the lower strength and/or stiffness range of the scatter. If the sample chosen is on the higher end of the spectrum, with higher material properties, the fatigue life is longer, and the damage accumulation is extensive and progressive, involving a number of mechanisms in addition to simple catastrophic composite failure. This pattern is further exemplified by failures occurring in regions of the structure where the stress levels are below the maximum as a result of weak locations. Overall, this extensive scatter in material properties poses new challenges to evaluating the failure mechanisms exhibited during bending tests on hat sections and other structural components. The challenge will be even greater for the future modeling effort, which will strive to accurately and

efficiently represent the behavior of a structure made from this material.

In addition to the nonhomogeneous properties inherent in the chosen composite material system, it was observed that measurable displacements could be tracked over time at relatively low-load levels below the damage threshold. Future testing will reveal if the scatter and variation in specimen stiffness play a significant role in creep response, or if they are periodic within the hybrid-joint structure to the extent of being smeared out or producing an average response for the structure below the damage levels. Additional replicate tests are being conducted to determine the levels of scatter among creep specimens.

Quasi-static cold testing of the hybrid rail specimens revealed a marked increase in strength. It may be due to a shifting of yield points in both the steel and the composite and stiffness changes in the composite. Additional coupon tensile testing in the cold environment will provide further information concerning composite behavior under this condition.